

# Optical study of electron-electron exchange interaction in CdTe/ZnTe quantum dots

T. Kazimierczuk,<sup>1,\*</sup> T. Smoleński,<sup>1</sup> J. Kobak,<sup>1</sup> M. Goryca,<sup>1</sup> W. Pacuski,<sup>1</sup>  
A. Golnik,<sup>1</sup> K. Fronc,<sup>2</sup> L. Kłopotowski,<sup>2</sup> P. Wojnar,<sup>2</sup> and P. Kossacki<sup>1</sup>

<sup>1</sup>*Institute of Experimental Physics, Faculty of Physics, University of Warsaw,  
Hoża 69, 00-681 Warsaw, Poland*

<sup>2</sup>*Institute of Physics, Polish Academy of Sciences,  
Al. Lotników 32/64, 02-688 Warsaw, Poland*

(Dated: August 14, 2018)

We present an experimental study of electron-electron exchange interaction in self-assembled CdTe/ZnTe quantum dots based on the photoluminescence measurements. The character and strength of this interaction are obtained by simultaneous observation of various recombination channels of a doubly negatively charged exciton  $X^{2-}$ , including previously unrecognized emission lines related to the electron-singlet configuration in the final state. A typical value of the electron singlet-triplet splitting, which corresponds to the exchange integral of electron-electron interaction, has been determined as 20.4 meV with a spread of 1.4 meV across the wide population of quantum dots. We also evidence an unexpected decrease of energy difference between the singlet and triplet states under a magnetic field in Faraday geometry.

PACS numbers: 78.55.Et, 78.67.Hc, 71.70.Gm

## I. INTRODUCTION

Semiconductor quantum dots (QDs) with their ability to confine carriers create convenient conditions to study various interactions between confined quasi-particles, in particular the exchange interaction. Experimentally, polarization-resolved spectroscopy provides a relatively easy access to the exchange interaction between an electron and a hole.<sup>1</sup> Due to heavy-hole character of the exciton ground state in a QD, the effective electron-hole exchange interaction is Ising-like (described by the so-called isotropic exchange constant  $\delta_0$ ) with a weak perturbation related to the QD in-plane anisotropy (described by anisotropic exchange constants  $\delta_1$  and  $\delta_2$ ).

In contrast to the electron-hole interaction, the exchange interaction between two electrons is much closer to the picture of two simple 1/2-spin particles and thus leads to the formation of singlet and triplet configurations. Such a singlet-triplet structure was mostly studied in the coupled dot pairs<sup>2</sup>. Observation of the effects related to the singlet-triplet structure in a single self-assembled QD is more difficult. Such effects manifest themselves only in the properties of the excited excitonic complexes. Emergence of singlet-triplet structure requires the presence of two electrons occupying different orbitals, e.g., one electron occupying the  $s$ -shell orbital, and the other one the  $p$ -shell orbital. The simplest excitonic complexes with such carriers are the excited negatively charged exciton ( $X^{-*}$ ) and the doubly negatively charged exciton ( $X^{2-}$ ) in the fundamental state. The properties of electron-electron interaction can be accessed by studying different recombination channels of an  $X^{2-}$  complex<sup>3-6</sup> or the photoluminescence excitation (PLE) of negatively charged dots<sup>7</sup>. The values of  $s$ - $p$  electron-electron exchange integral reported in previous studies vary from about 4 meV<sup>4</sup> for InAs/GaAs QDs, to nearly 80 meV<sup>7</sup> in the case of CdSe/ZnSe QDs.

In this paper we present a spectroscopic study of emission lines related to different recombination channels of a doubly negatively charged exciton  $X^{2-}$  confined in self-assembled CdTe/ZnTe QD. The final states of identified transitions correspond to the excited state of two electrons forming either a singlet or a triplet configuration. We discuss the anisotropy-related fine structure of these transitions as well as their behavior in an external magnetic field, both in Faraday and Voigt configurations. We demonstrate that the properties of observed transitions can be understood within the frame of a simple spin Hamiltonian previously used to describe  $X^{2-}$  and  $XX^{-}$  recombination to the triplet final state<sup>8</sup>. We also point out deficiencies of such a simple model, namely incorrect predictions of the relative intensities of optical transitions to the singlet final state and the effects related to singlet-triplet splitting in the magnetic field. Moreover, we propose an explanation of the former shortcoming as originating from the presence of configuration mixing in a QD, the importance of which was already shown in several previous studies.<sup>9,10</sup>

## II. SAMPLES AND EXPERIMENTAL SETUP

The measurements were performed on samples containing a single layer of self-organized CdTe QDs embedded in a ZnTe matrix. The samples were grown by molecular beam epitaxy (MBE). The QD formation was induced by temporary covering the CdTe formation layer with amorphous tellurium, as described in Refs. 11,12. The spectroscopy of single quantum dots over a wide range of emission energies was achieved by collecting the light through nanometer-size shadow mask apertures on a sample surface. The apertures were manufactured by depositing a nontransparent 100nm layer of gold onto a sample with spin-casted 200 nm polystyrene beads,

which were afterwards removed by ultrasonic rinsing in trichloroethylene and methanol.

The measurements were carried out in a high-resolution spectroscopy setup with a laser spot of diameter corresponding to about  $0.5 \mu\text{m}$ . The PL was excited non-resonantly at 400 nm. The signal was resolved using a 0.5-m monochromator and recorded using a CCD camera. The samples were placed in a helium-bath cryostat at temperature of 1.5 K. The cryostat was equipped with a split-coil superconducting magnet producing magnetic field up to 11T in Faraday or Voigt geometry. More details about the samples and the experimental setup can be found in Refs. 8,13.

### III. POLARIZATION-RESOLVED PHOTOLUMINESCENCE OF CDTE/ZNTE QDS

Basic properties of measured single QDs PL spectra fully reproduce the findings of previous studies of CdTe based dots.<sup>8,14-16</sup> The PL spectrum of a single randomly selected QD [presented in Fig 1(a)] consists of a number of sharp emission lines originating from recombination of different excitonic complexes. Due to the high efficiency of single carrier capture under nonresonant excitation<sup>14</sup>, we observe emission lines related to the transitions of excitons of various charge states. The sequence and the relative energies of the emission lines were shown to be similar for different self-assembled CdTe/ZnTe QDs<sup>8</sup>. On this basis we identify the strongest emission lines in the spectrum presented in Fig. 1(a) as related to the recombination of neutral exciton (X), positively and negatively charged excitons ( $X^+$ ,  $X^-$ ), doubly negatively charged exciton ( $X^{2-}$ ), neutral biexciton (XX), and negatively charged biexciton ( $XX^-$ ). Most of these transitions exhibit non-trivial fine structure due to the presence of exchange interaction between confined carriers<sup>1,8</sup>. Analysis of this fine structure is a potent tool in identification of the emission lines in single dot PL spectrum. A well known example is distinguishing between neutral and charged exciton<sup>1</sup>. Here we use the analysis of the fine structure to argue that despite the surprisingly large spectral distance, a previously unrecognized pair of lines denoted in Fig. 1 as  $X_s^{2-}$  does in fact originate from the same QD and is related to the recombination of doubly charged exciton to the two-electron singlet state.

The analysis of the fine structure benefits from the fact that in the typical case, the exchange interaction between electrons and holes has anisotropic character. This anisotropy is manifested by the linear polarization of the light emitted during recombination of fine-structure-split excitonic complexes. Previous studies revealed that different emission lines of the same quantum dot can exhibit different polarization axes<sup>5,8</sup>, especially when they originate from recombination of excitonic complexes consisting of carriers occupying the higher shells. As a consequence, the polarization-resolved experiment cannot be reduced to measurements of PL signal in two orthogonal

linear polarizations. Instead, the intensity of each emission line needs to be analyzed for a number of different polarizations in order to determine the orientation of polarization related to a given transition. Figure 1(b) shows PL spectra of a single QD measured for a whole range of orientations of detected linear polarization. Due to relatively small splitting, the fine structure of the neutral exciton is visible here only as a small modulation of the average energy of X (and XX) emission line. Nevertheless, the intensities of both fine-split components of X could be extracted by fitting the emission line with two Gaussian profiles of fixed positions. In the same way we also extracted the angle-dependent intensities of other emission lines, including  $X_s^{2-}$  lines as well. Angular dependence of the intensity of the relevant lines is presented in Figs. 1(c)-1(e). As expected, in each case the anisotropic electron-hole exchange interaction led to splitting of the emission line into two components of orthogonal linear polarizations. Possible deviation from the orthogonality of these linear polarizations is introduced by the valence band mixing<sup>17-19</sup>, which for the QD in Fig. 1 was found to be smaller than 3%.

The QD shown in Fig. 1 exhibits a difference between orientations of the polarization of the neutral exciton X (here,  $32^\circ$ ) and the doubly charged exciton  $X^{2-}$  (here:  $11^\circ$ ). Interestingly, the orientation of the latter one exactly (with precision better than  $1^\circ$ ) matches the fine structure of the previously unrecognized  $X_s^{2-}$  doublet. Moreover both complexes —  $X^{2-}$  and  $X_s^{2-}$  — exhibit practically equal fine structure splittings of 0.53 meV. Such a coincidence strongly suggests existence of a link between  $X^{2-}$  and  $X_s^{2-}$ . These observations are not specific only to the presented QD. In the following section we argue that these properties are characteristic for the recombination of a doubly charged exciton  $X^{2-}$  to the state with two electrons in a singlet configuration (as opposed to the previously recognized recombination to triplet configuration) and compare the predictions of the model calculations with the measurements on a population of 18 different QDs.

### IV. PREDICTIONS REGARDING $X^{2-}$ TRANSITION WITHIN SPIN HAMILTONIAN MODEL

The simplest and the most transparent way to model the recombination of doubly charged exciton is to use simple spin Hamiltonian. The model assumes that the spin-related interactions between confined carriers are weak in comparison with the spatial confinement. In such a case, the carriers populate subsequent orbitals according to the aufbau principle, and the exchange interaction is used only to determine the fine structure within otherwise degenerate subspace.

The description of doubly charged exciton  $X^{2-}$  required using three types of carriers:  $s$ -shell hole,  $s$ -shell electron, and  $p$ -shell electron. For simplicity, we assume

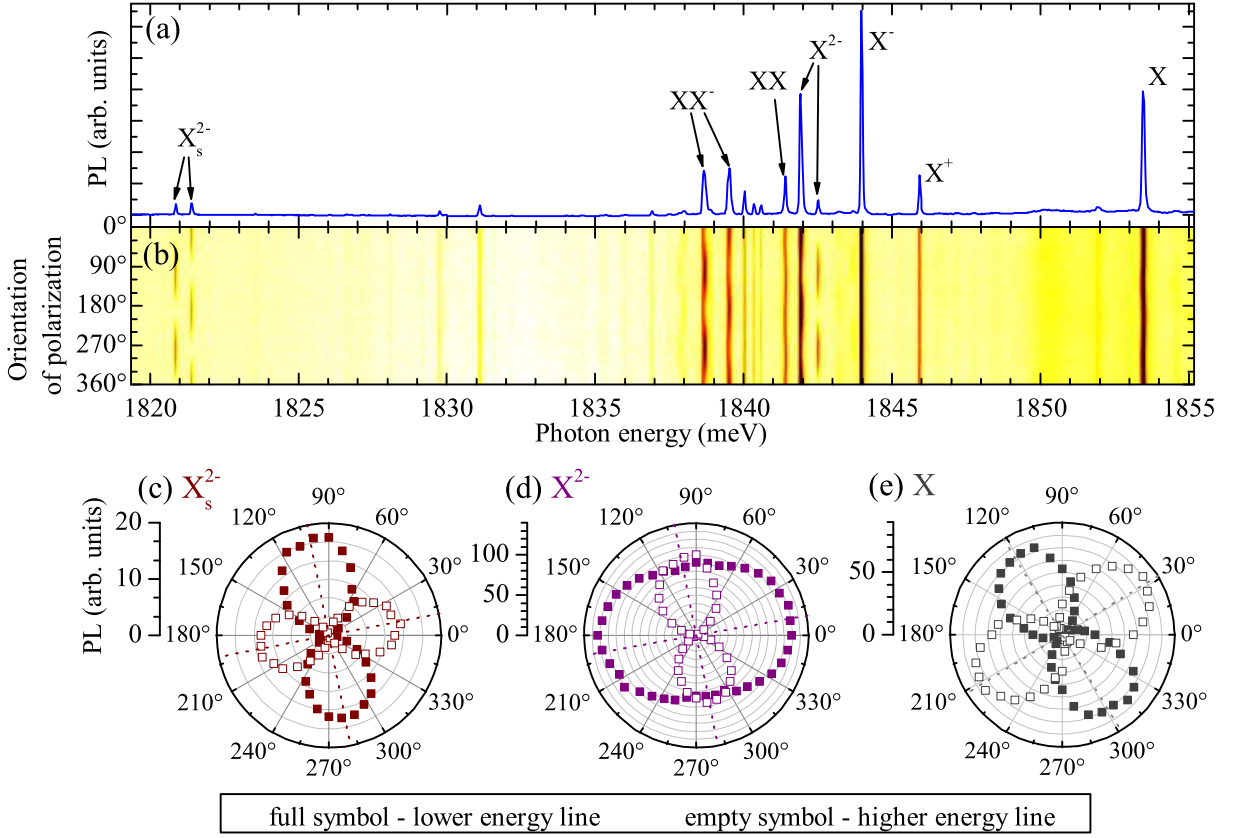


FIG. 1: (Color online) (a) Photoluminescence spectrum of a single CdTe/ZnTe QD without polarization resolution. Lines denoted by  $X_s^{2-}$  correspond to recombination of a doubly charged exciton to a state with two electrons in singlet configuration. (b) False-color plot presenting PL spectra of the same QD measured using different linear polarization of detection. The  $0^\circ$  and  $90^\circ$  correspond to cleavage axes of the sample. (c-e) Dependence of the PL intensity of  $X_s^{2-}$ ,  $X^{2-}$ , and  $X$  doublets on the orientation of detected polarization for the same QD. In case of  $X^{2-}$ , the lower energy line exhibit only partial linear polarization due to the coincidental contribution from unpolarized transition<sup>8</sup>. The intensity of the higher energy component of  $X^{2-}$  was magnified by a factor 4 for better visibility.

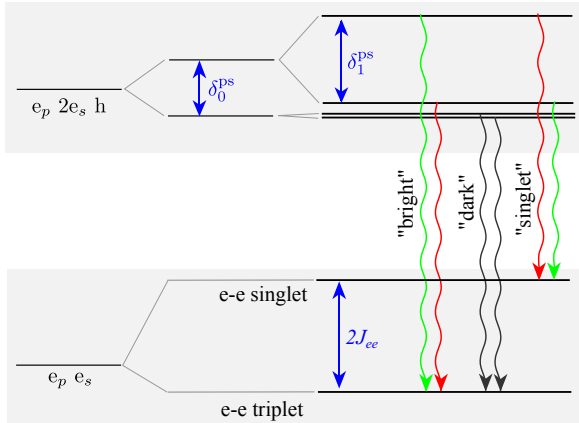


FIG. 2: (Color online) A scheme of states and transitions related to the recombination of doubly charged exciton  $X^{2-}$ . Note that the level spacing is not in scale. Colors of the arrows denote polarization of the transition. Red and green (different shades of light grey) denote orthogonal linear polarization while dark grey denotes unpolarized transition.

the presence of only one lowest  $p$  orbital, possibly due to the anisotropy of the dot. Each pair of the carriers interact by the exchange interaction. The interaction between  $s$ - or  $p$ -shell electron with the hole includes both iso- and anisotropic parts<sup>3,6,8,20</sup>:

$$H_1 = 2\delta_0 S_z^{(s)} \sigma_z + \delta_1 \left( S_x^{(s)} \sigma_x - S_y^{(s)} \sigma_y \right), \quad (1)$$

$$H_2 = 2\delta_0^{(ps)} S_z^{(p)} \sigma_z + \delta_1^{(ps)} \left( S_x^{(p)} \sigma_x - S_y^{(p)} \sigma_y \right), \quad (2)$$

where  $S^{(s)}$ ,  $S^{(p)}$ , and  $\sigma$  are the spin operators for  $s$ -shell electron,  $p$ -shell electron, and the hole respectively. In case of the hole, we use pseudo-spin convention, i.e., we formally treat the  $\pm 3/2$  heavy hole states as  $\mp 1/2$  pseudo-spin states. The inter-shell electron-electron exchange interaction is assumed to have purely isotropic character, as the experimental data do not indicate such an anisotropy:

$$H_3 = -2J_{ee} \vec{S}^{(s)} \vec{S}^{(p)}. \quad (3)$$

The final Hamiltonian is a sum of such contributions for each pair of confined carriers. In the presence of an external magnetic field, additional terms of the form  $g\mu_B BS$  are added for each confined carrier.

The initial state of transition consists of three electrons and one hole. Two electrons fully occupy the  $s$ -shell and the remaining electron is placed on the  $p$ -shell. As a result, there are four base spin configurations of an initial excitonic complex with two possible spin orientations of the hole as well as the  $p$ -shell electron. The degeneracy of these four states is lifted by the exchange interaction between the unpaired carriers. In this respect, there is a close analogy between a neutral exciton (with a single electron on the  $s$  shell) and doubly charged exciton (with a single electron on the  $p$  shell). Consequently, the eigenstates of doubly charged exciton take the form

$$\begin{aligned} & \frac{1}{\sqrt{2}} \left( \left| \begin{smallmatrix} \uparrow \\ \uparrow \downarrow \end{smallmatrix} \downarrow \right\rangle + \left| \begin{smallmatrix} \downarrow \\ \uparrow \downarrow \end{smallmatrix} \uparrow \right\rangle \right), \quad \frac{1}{\sqrt{2}} \left( \left| \begin{smallmatrix} \uparrow \\ \uparrow \downarrow \end{smallmatrix} \downarrow \right\rangle - \left| \begin{smallmatrix} \downarrow \\ \uparrow \downarrow \end{smallmatrix} \uparrow \right\rangle \right), \\ & \frac{1}{\sqrt{2}} \left( \left| \begin{smallmatrix} \uparrow \\ \uparrow \downarrow \end{smallmatrix} \uparrow \right\rangle + \left| \begin{smallmatrix} \downarrow \\ \uparrow \downarrow \end{smallmatrix} \downarrow \right\rangle \right), \quad \frac{1}{\sqrt{2}} \left( \left| \begin{smallmatrix} \uparrow \\ \uparrow \downarrow \end{smallmatrix} \uparrow \right\rangle - \left| \begin{smallmatrix} \downarrow \\ \uparrow \downarrow \end{smallmatrix} \downarrow \right\rangle \right), \end{aligned}$$

where  $\left| \begin{smallmatrix} A \\ B \\ C \end{smallmatrix} \right\rangle$  denotes a state with  $A$  electron(s) on the  $p$  shell,  $B$  electron(s) on the  $s$  shell and  $C$  hole(s) on the  $s$  shell.  $\uparrow$  and  $\downarrow$  represent  $\pm 1/2$  electron spin, while  $\uparrow$  and  $\downarrow$  represent  $\pm 3/2$  heavy-hole spin. The first and the second of the four states are the analogs of the bright states of the neutral exciton. They are split by anisotropic inter-shell exchange constant  $\delta_1^{\text{ps}} \approx -0.5$  meV<sup>8</sup>. The third and the fourth of these states are analogs of the dark states of the neutral exciton. The splitting between two “dark” states can be neglected in our dots. Both pairs, “bright” and “dark” states are split by isotropic inter-shell exchange constant  $\delta_0^{\text{ps}} \approx 0.3$  meV<sup>8</sup>.

In the final state of the transitions two electrons are left in the QD: one on the  $s$  shell and one on the  $p$  shell. These two electrons interact with the exchange interaction, thus the eigenstates take a form of singlet-triplet structure:

$$\begin{aligned} |S\rangle &= \frac{1}{\sqrt{2}} \left( \left| \begin{smallmatrix} \downarrow \\ \uparrow \end{smallmatrix} \right\rangle - \left| \begin{smallmatrix} \uparrow \\ \downarrow \end{smallmatrix} \right\rangle \right), \\ |T_1\rangle &= \left| \begin{smallmatrix} \uparrow \\ \uparrow \end{smallmatrix} \right\rangle, |T_0\rangle = \frac{1}{\sqrt{2}} \left( \left| \begin{smallmatrix} \downarrow \\ \uparrow \end{smallmatrix} \right\rangle + \left| \begin{smallmatrix} \uparrow \\ \downarrow \end{smallmatrix} \right\rangle \right), |T_{-1}\rangle = \left| \begin{smallmatrix} \downarrow \\ \downarrow \end{smallmatrix} \right\rangle. \end{aligned}$$

Optical selection rules require antiparallel spin orientation of recombining electron-hole pair. Moreover, due to symmetry difference between  $s$ - and  $p$ -shell, only  $s$ -shell electrons can recombine with the  $s$ -shell hole. Even if this restriction is partially lifted by imperfections of the real QD potential, the assumed recombination of  $s$ -shell electron should be significantly stronger than recombination involving  $p$ -shell electron. More importantly, recombination of  $p$ -shell electron would produce emission lines at higher energy than other emission lines in the studied PL spectrum, which we do not find in the experiment.

Discussed selection rules constraints are met by three sets of transitions. The first group of transitions is related to initial states being the analogs of the dark states of a neutral excitons (i.e., the unpaired electron and the hole

have parallel spin orientation). Consequently we will refer to these transitions using label “dark”, irrespectively of the actual strength of these transitions. According to the selection rules, the  $s$ -shell electron remaining after recombination has the same orientation of the spin as the recombining hole, which for “dark” state is the same as the  $p$ -shell electron. Consequently, the allowed final states of the transition are  $S = \pm 1$  states of the triplet with two parallel electron spins:

$$\begin{aligned} & \frac{1}{\sqrt{2}} \left( \left| \begin{smallmatrix} \uparrow \\ \uparrow \downarrow \end{smallmatrix} \uparrow \right\rangle + \left| \begin{smallmatrix} \downarrow \\ \uparrow \downarrow \end{smallmatrix} \downarrow \right\rangle \right) \xrightarrow{\text{“dark”}} \left| \begin{smallmatrix} \uparrow \\ \uparrow \end{smallmatrix} \right\rangle \text{ or } \left| \begin{smallmatrix} \downarrow \\ \downarrow \end{smallmatrix} \right\rangle, \\ & \frac{1}{\sqrt{2}} \left( \left| \begin{smallmatrix} \uparrow \\ \uparrow \downarrow \end{smallmatrix} \uparrow \right\rangle - \left| \begin{smallmatrix} \downarrow \\ \uparrow \downarrow \end{smallmatrix} \downarrow \right\rangle \right) \xrightarrow{\text{“dark”}} \left| \begin{smallmatrix} \uparrow \\ \uparrow \end{smallmatrix} \right\rangle \text{ or } \left| \begin{smallmatrix} \downarrow \\ \downarrow \end{smallmatrix} \right\rangle. \end{aligned}$$

Without magnetic field neither initial nor the final state of these transitions are split. As a result, these transitions contribute to a single non-polarized line in the PL spectrum.

The second and the third group of the transitions are related to recombination of the  $X^{2-}$  complex with anti-parallel spins of the  $p$ -shell electron and the hole. According to the selection rules, the electrons in the final state of the transition also have anti-parallel spin configuration which may indicate either the singlet state or the  $S = 0$  triplet state. A more strict approach<sup>8</sup> shows, that our model entails both possible final states. We will refer to the transitions leading to the triplet state using the label “bright” (again, with no reference to the transition strength), while the transitions leading to the singlet state will be referred to simply as “singlet”:

$$\begin{aligned} & \frac{1}{\sqrt{2}} \left( \left| \begin{smallmatrix} \uparrow \\ \uparrow \downarrow \end{smallmatrix} \downarrow \right\rangle + \left| \begin{smallmatrix} \downarrow \\ \uparrow \downarrow \end{smallmatrix} \uparrow \right\rangle \right) \xrightarrow{\text{“bright”}} \frac{1}{\sqrt{2}} \left( \left| \begin{smallmatrix} \uparrow \\ \downarrow \end{smallmatrix} \right\rangle + \left| \begin{smallmatrix} \downarrow \\ \uparrow \end{smallmatrix} \right\rangle \right), \\ & \frac{1}{\sqrt{2}} \left( \left| \begin{smallmatrix} \uparrow \\ \uparrow \downarrow \end{smallmatrix} \downarrow \right\rangle - \left| \begin{smallmatrix} \downarrow \\ \uparrow \downarrow \end{smallmatrix} \uparrow \right\rangle \right) \xrightarrow{\text{“bright”}} \frac{1}{\sqrt{2}} \left( \left| \begin{smallmatrix} \uparrow \\ \downarrow \end{smallmatrix} \right\rangle + \left| \begin{smallmatrix} \downarrow \\ \uparrow \end{smallmatrix} \right\rangle \right), \\ & \frac{1}{\sqrt{2}} \left( \left| \begin{smallmatrix} \uparrow \\ \uparrow \downarrow \end{smallmatrix} \downarrow \right\rangle + \left| \begin{smallmatrix} \downarrow \\ \uparrow \downarrow \end{smallmatrix} \uparrow \right\rangle \right) \xrightarrow{\text{“singlet”}} \frac{1}{\sqrt{2}} \left( \left| \begin{smallmatrix} \uparrow \\ \downarrow \end{smallmatrix} \right\rangle - \left| \begin{smallmatrix} \downarrow \\ \uparrow \end{smallmatrix} \right\rangle \right), \\ & \frac{1}{\sqrt{2}} \left( \left| \begin{smallmatrix} \uparrow \\ \uparrow \downarrow \end{smallmatrix} \downarrow \right\rangle - \left| \begin{smallmatrix} \downarrow \\ \uparrow \downarrow \end{smallmatrix} \uparrow \right\rangle \right) \xrightarrow{\text{“singlet”}} \frac{1}{\sqrt{2}} \left( \left| \begin{smallmatrix} \uparrow \\ \downarrow \end{smallmatrix} \right\rangle - \left| \begin{smallmatrix} \downarrow \\ \uparrow \end{smallmatrix} \right\rangle \right). \end{aligned}$$

All these transitions are depicted in Fig. 2. The spin Hamiltonian model predicts that “singlet” transitions should be present in the PL spectrum as a pair of lines with exactly the same splitting as “bright” transitions ( $\delta_1^{\text{ps}}$ ). In both cases the split lines exhibit orthogonal linear polarizations. The orientation of this linear polarization is governed by the (common) initial state of the transition and therefore should be the same for “singlet” and “bright” transitions. However, due to different symmetry of the final states, the order of the polarizations is reversed. The lower energy line of “singlet” transition has the same polarization as higher energy line of “bright” transition and *vice versa*.

These predictions are fully confirmed by the experimental data, as shown in Fig. 3. Despite random distribution of the polarization angle or the value of the splitting, for each studied QD “singlet” transition exhibited the same splitting and opposite linear polarizations as “bright” recombination of  $X^{2-}$ . Such a good agreement is an unequivocal confirmation of correct identification

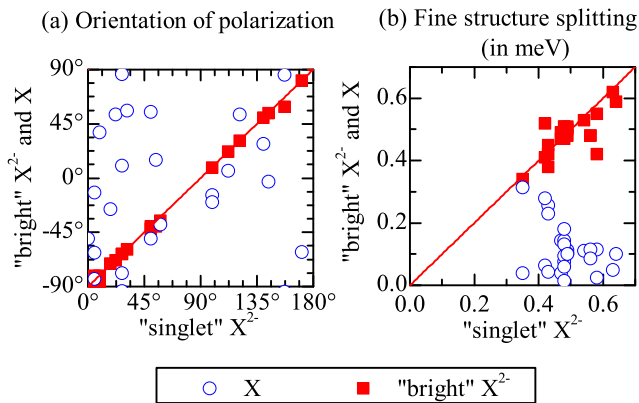


FIG. 3: (Color online) Correlation of (a) orientations of polarization and (b) splittings of doubly charged exciton  $X^{2-}$  for different QDs (red squares). Blue circles represent analog data for the neutral exciton for comparison. Solid line corresponds to the predictions of the spin Hamiltonian model, namely  $90^\circ$  difference in orientation of polarization and the same splitting of "bright" and "singlet" transitions.

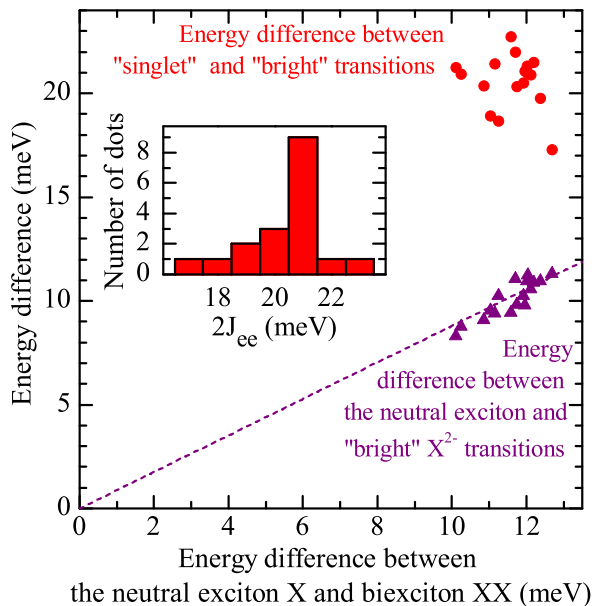


FIG. 4: (Color online) Correlation of relative spectral line positions. The relative position of "bright" and "dark" transitions is proportional to the relative position of the other lines of the same QD (e.g., neutral biexciton), while the splitting between singlet and triplet ( $2J_{ee}$ ) seems to be independent of these relative positions. The inset presents a histogram of  $2J_{ee}$  constant among studied dots.

of line  $X_s^{2-}$  from Fig. 1 as a "singlet" recombination channel for doubly charged exciton  $X^{2-}$ .

Simultaneous observation of both "singlet" and "bright" transition lines opens a possibility to determine a strength of electron-electron exchange constant  $J_{ee}$ . The value determined by averaging a distance between "singlet" and "bright" emission lines for 18 different QDs

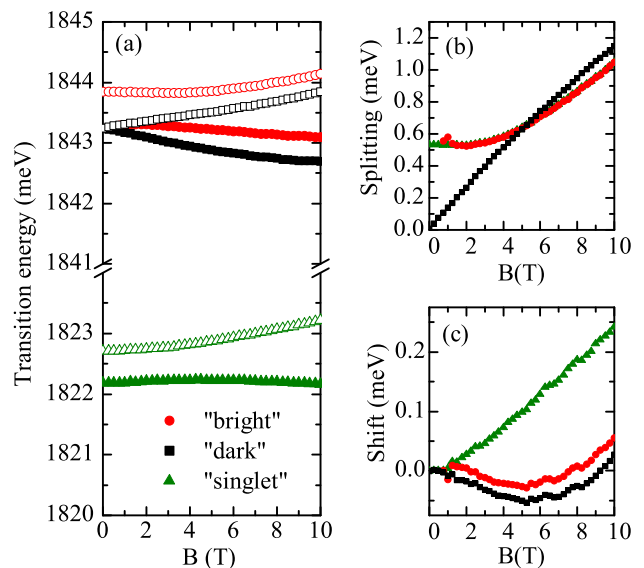


FIG. 5: (Color online) (a) Magnetic field dependence of transition energies in Faraday configuration. Empty (full) symbols denote lines with  $\sigma+$  ( $\sigma-$ ) helicity. The same data was used to calculate (b) Zeeman splitting and (c) diamagnetic shift for each pair of lines.

yielded  $2J_{ee} = (20.4 \pm 1.4)$  meV. Interestingly, this quantity does not scale with energy distances between other lines, which otherwise vary proportionally from dot to dot<sup>8</sup> in our samples. It is shown in Fig. 4, where clear proportionality between energy distances from X to XX and from X to "bright" transition of  $X^{2-}$  contrasts with a lack of correlation for  $J_{ee}$  value.

We also stress out, that our measurements do not indicate the presence of the anisotropic part of electron-electron exchange interaction, which was anticipated in Ref. 21. Such an anisotropy of the exchange interaction would lift the degeneracy between  $T_0$  and  $T_{\pm 1}$  states. In such a scenario the higher-energy "bright" line would be a transition from non-degenerate initial state to non-degenerate final state and thus cannot exhibit any splitting. However, the measurements reported earlier in Ref. 8 clearly show two-fold linear splitting of this emission line in the magnetic field in the Voigt geometry. Observed behavior is a clear proof of degeneracy of  $T_0$  and  $T_{\pm 1}$  states at  $B = 0$ , which indicates purely isotropic character of the electron-electron exchange interaction.

## V. DOUBLY CHARGED EXCITON IN MAGNETIC FIELD

In order to provide additional information about studied transitions, we measured the magnetic field dependence of all transitions related to recombination of doubly charged exciton. Results of such an experiment in Faraday configuration are shown in Fig. 5.

Under magnetic field along the growth axis, we ob-

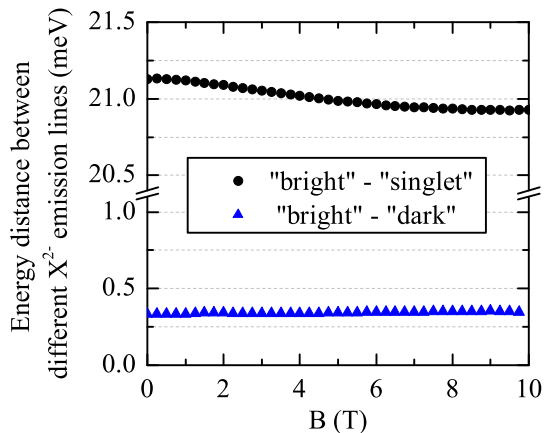


FIG. 6: (Color online) Energy distances between various pairs of emission lines related to  $X^{2-}$  recombination in magnetic field in Faraday geometry. Energy of each pair is defined by the average of both components using data from Fig. 5(a). Due to common initial state, "bright"-singlet distance is a direct measure of splitting between singlet and triplet  $T_0$  configuration of two electrons.

served clear splitting of each set of transitions ("bright", "dark", and "singlet") into two lines of opposite helicity of polarization. For "bright" and "singlet" transitions, the degree of circular polarization was increasing with field intensity, while "dark" transitions exhibited full circular polarization even in moderate magnetic field. Indeed, according to our model, magnetic field in Faraday configuration does not couple "bright" and "dark" initial states nor singlet-triplet final states. As a result, effect of the magnetic field can be analyzed separately for each pair of  $X^{2-}$  transitions lines.

We first focus on the splitting of each pair of lines [see Fig. 5(b)]. Two main contributions to this splitting are the zero-field fine structure splitting and the Zeeman contribution. As discussed earlier, the fine structure splitting is present for both "bright" and "singlet" lines, while "dark" transitions do not exhibit observable zero-field splitting. Under influence of the field, the splitting of each line increases according to the relation  $\sqrt{\Delta^2 + (g\mu_B B)^2}$ , where  $\Delta$  is corresponding zero-field splitting. As reported previously<sup>22</sup>, we find different effective  $g$ -factor values for the "bright" and "dark" transitions, which we interpret as a signature of difference in  $g$ -factors for  $s$ - and  $p$ -shell electrons. In comparison, we find the field dependence of the splitting of the "singlet" lines to perfectly follow the dependence of the splitting of the "bright" lines. This is another confirmation of the fact, that both of these pairs of transitions originate from the same initial states and lead to a single (but different in each case) final state.

## VI. BEYOND THE SPIN HAMILTONIAN MODEL

This close connection between the "singlet" and "bright" transitions allows us to directly measure the electron singlet-triplet energy distance as a function of the magnetic field. In principle, neither the electron singlet nor the triplet  $T_0$  state should be affected by the magnetic field. However, the experimental results shown in Fig. 6 indicate that magnetic field leads to a small reduction in the distance between the energy of electron singlet state and triplet  $T_0$  state. The presence of this effect was confirmed by repeating the experiment on several other QDs. The physical origin of the observed variation is not fully understood. Possibly, the effect is due to different diamagnetic shift of the singlet and triplet state. Increased spatial extension of the electron singlet state due to additional exchange energy would lead to greater diamagnetic shift and thus would reduce the energy difference between the singlet and triplet state. However, the range of magnetic field available in our experiments do not allow us to unequivocally verify this hypothesis.

The second notable difference between the predictions of the simple spin Hamiltonian model and the experimental data is related to relative intensities of different  $X^{2-}$  emission lines. In particular, the "singlet" and "bright" transitions originate from the same initial states and therefore their relative intensities do not depend on the QD excitation but they are governed solely by the relative strength of dipole moment for these transitions. The spin Hamiltonian model assumes that the spatial part of the wavefunction is the same in all engaged states and thus the transition moments are defined by the projection of the spin part of the wavefunction onto possible final eigenstates. As such, the model predicts equal strength of "singlet" and "bright" transitions. On the contrary, the experimental data evidence a significant systematic difference between intensities of the emission lines related to "singlet" and "bright" transitions, as shown in Fig. 7. In order to understand the possible origins of such a difference, we performed calculations of oscillator strengths of  $X^{2-}$  optical transitions within the frame of an extended theoretical model, which takes into account the configuration mixing<sup>9,10</sup>. In contrast to the previously exploited simple spin Hamiltonian model, the current one includes the mixing between the many-particle states consisting of the same number of electrons and holes, which occupy different QD shells. Therefore, in the extended model the spatial parts of the wavefunctions of  $X^{2-}$  recombination final states can in principle be different, and thus the predicted strengths of "singlet" and "bright" transitions may not be equal. Such an analysis is carried out by detailed numerical calculations performed in the basis of many-particle states involving three lowest QD shells (i.e., up to  $d$ -shell), for typical CdTe/ZnTe QD parameters described in Ref. 10. As a result we obtained the ratio of "singlet" and "bright" transitions strength to be about 0.5, which is much closer to the experimentally



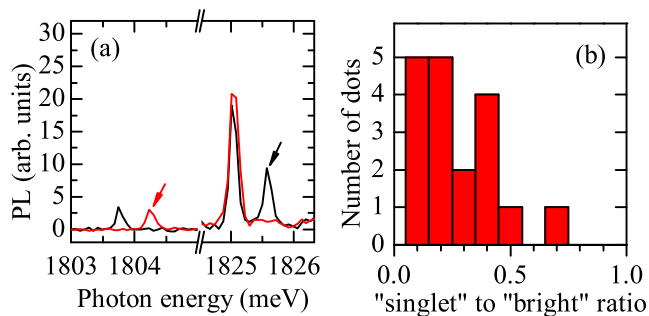


FIG. 7: (Color online) (a) Photoluminescence spectrum with emission lines related to different recombination channels of  $X^{2-}$  measured in two orthogonal linear polarizations. Arrows point the transitions originating from the same initial state either to singlet or triplet configuration. The intensities of these two channels should be equal according to the spin hamiltonian model. The actual intensity of the “singlet” transition for this dot is only 0.45 of the intensity of the “bright” transition. (b) Histogram of ratio between intensities of “singlet” and “bright” emission lines for different QDs. The average ratio for the studied population was 0.28.

obtained values (see Fig. 7). However, the ratio given by the extended model still does not reach the measured values, which indicates the need for further investigation of that effect.

## VII. CONCLUSIONS

In conclusion, we characterized the interaction between two electrons in CdTe/ZnTe QDs based on the results of

the single dot PL measurements. The two electron states were accessed by analysis of emission lines related to three different recombination channels of doubly charged exciton  $X^{2-}$ . Two of the channels (labeled as “bright” and “dark”) lead to the triplet configuration of remaining electrons, and the third one (labeled as “singlet”) leads to the singlet configuration. By identification of all these transitions in a single dot PL spectrum we evaluated the basic quantity describing electron-electron exchange interaction in our CdTe/ZnTe QDs, namely the exchange constant  $2J_{ee} = (20.4 \pm 1.4)$  meV. We did not find any fingerprints of anisotropic contribution to the electron-electron interaction. Moreover, we found that the energy splitting between the singlet and the triplet state is reduced by external magnetic field parallel to the growth axis. The origin of this effect is not fully understood yet. Some light on this origin might be shed by the quantitative modeling of CdTe/ZnTe QDs, which in turn can benefit from our findings on electron-electron exchange interaction in this system.

### Acknowledgments

This work was supported by the Polish Ministry of Science and Higher Education in years 2012–2016 as research grants “Iuventus” and a “Diamentowy Grant”, NCBiR project LIDER, and NCN projects DEC-2011/01/B/ST3/02406 and DEC-2011/02/A/ST3/00131. Experiments were carried out with the use of CePT, CeZa-Mat and NLTK infrastructures financed by the European Union - the European Regional Development Fund within the Operational Programme “Innovative economy” for 2007–2013.

\* Electronic address: Tomasz.Kazimierczuk@fuw.edu.pl

<sup>1</sup> M. Bayer, G. Ortner, O. Stern, A. Kuther, A. A. Gorbunov, A. Forchel, P. Hawrylak, S. Fafard, K. Hinzer, T. L. Reinecke, et al., Phys. Rev. B **65**, 195315 (2002).  
<sup>2</sup> A. C. Johnson, J. R. Petta, C. M. Marcus, M. P. Hanson, and A. C. Gossard, Phys. Rev. B **72**, 165308 (2005).  
<sup>3</sup> B. Urbaszek, R. J. Warburton, K. Karrai, B. D. Gerardot, P. M. Petroff, and J. M. Garcia, Phys. Rev. Lett. **90**, 247403 (2003).  
<sup>4</sup> J. J. Finley, P. W. Fry, A. D. Ashmore, A. Lemaître, A. I. Tartakovskii, R. Oulton, D. J. Mowbray, M. S. Skolnick, M. Hopkinson, P. D. Buckle, et al., Phys. Rev. B **63**, 161305 (2001).  
<sup>5</sup> E. Poem, J. Shemesh, I. Marderfeld, D. Galushko, N. Akopian, D. Gershoni, B. D. Gerardot, A. Badolato, and P. M. Petroff, Phys. Rev. B **76**, 235304 (2007).  
<sup>6</sup> M. Ediger, G. Bester, B. D. Gerardot, A. Badolato, P. M. Petroff, K. Karrai, A. Zunger, and R. J. Warburton, Phys. Rev. Lett. **98**, 036808 (2007).  
<sup>7</sup> I. A. Akimov, T. Flissikowski, A. Hundt, and F. Henneberger, Phys. Stat. Sol. (a) **201**, 412 (2004).  
<sup>8</sup> T. Kazimierczuk, T. Smoleński, M. Goryca, L. Kłopotowski, P. Wojnar, K. Fronc, A. Golnik,

M. Nawrocki, J. A. Gaj, and P. Kossacki, Phys. Rev. B **84**, 165319 (2011).

<sup>9</sup> P. Hawrylak, Phys. Rev. B **60**, 5597 (1999).  
<sup>10</sup> T. Smolenski, T. Kazimierczuk, M. Goryca, P. Kossacki, J. A. Gaj, P. Wojnar, K. Fronc, M. Korkusinski, and P. Hawrylak, Acta Phys. Pol. A **119**, 615 (2011).  
<sup>11</sup> F. Tinjod, B. Gilles, S. Moehl, K. Kheng, and H. Mariette, Appl. Phys. Lett. **82**, 4340 (2003).  
<sup>12</sup> P. Wojnar, J. Suffczyński, K. Kowalik, A. Golnik, M. Aleszkiewicz, G. Karczewski, and J. Kossut, Nanotechnology **19**, 235403 (2008).  
<sup>13</sup> T. Kazimierczuk, M. Goryca, M. Koperski, A. Golnik, J. A. Gaj, M. Nawrocki, P. Wojnar, and P. Kossacki, Phys. Rev. B **81**, 155313 (2010).  
<sup>14</sup> J. Suffczyński, T. Kazimierczuk, M. Goryca, B. Piechal, A. Trajnerowicz, K. Kowalik, P. Kossacki, A. Golnik, K. P. Korona, M. Nawrocki, et al., Phys. Rev. B **74**, 085319 (2006).  
<sup>15</sup> L. Besombes, K. Kheng, L. Marsal, and H. Mariette, Phys. Rev. B **65**, 121314 (2002).  
<sup>16</sup> L. Kłopotowski, V. Voliotis, A. Kudelski, A. I. Tartakovskii, P. Wojnar, K. Fronc, R. Grousson, O. Krebs, M. S. Skolnick, G. Karczewski, and T. Wojtowicz, Phys.

- Rev. B **83**, 155319 (2011).
- <sup>17</sup> Y. Léger, L. Besombes, L. Maingault, and H. Mariette, Phys. Rev. B **76**, 045331 (2007).
- <sup>18</sup> A. V. Koudinov, I. A. Akimov, Y. G. Kusrayev, and F. Henneberger, Phys. Rev. B **70**, 241305(R) (2004).
- <sup>19</sup> T. Smoleński, T. Kazimierzczuk, M. Goryca, T. Jakubczyk, L. Kłopotowski, L. Cywiński, P. Wojnar, A. Golnik, and P. Kossacki, Phys. Rev. B **86**, 241305(R) (2012).
- <sup>20</sup> I. A. Akimov, K. V. Kavokin, A. Hundt, and F. Henneberger, Phys. Rev. B **71**, 075326 (2005).
- <sup>21</sup> M. E. Ware, E. A. Stinaff, D. Gammon, M. F. Doty, A. S. Bracker, D. Gershoni, V. L. Korenev, S. C. Bădescu, Y. Lyanda-Geller, and T. L. Reinecke, Phys. Rev. Lett. **95**, 177403 (2005).
- <sup>22</sup> T. Kazimierzczuk, M. Goryca, P. Wojnar, A. Golnik, M. Nawrocki, and P. Kossacki, Acta Phys. Pol. A **120**, 874 (2011).